arXiv:1609.02547v1 [cond-mat.stat-mech] 8 Sep 2016

Steady-state skewness and kurtosis from renormalized cumulants in $(2+1)$-dimensional stochastic surface growth

Tapas Singha & Malay K. Nandy

Department of Physics, Indian Institute of Technology Guwahati, Guwahati 781039, India.

E-mail: s.tapas@iitg.ernet.in & mknandy@iitg.ernet.in

Abstract. The phenomenon of stochastic growth of a surface on a two-dimensional substrate occurs in Nature in a variety of circumstances and its statistical characterization requires the study of higher order cumulants. Here, we consider the statistical cumulants of height fluctuations governed by the $(2+1)$-dimensional KPZ equation for flat geometry. We follow a diagrammatic scheme to derive the expressions for renormalized cumulants up to fourth order in the stationary state. Assuming a value for the roughness exponent from reliable numerical predictions, we calculate the second, third and fourth cumulants, yielding skewness $S = 0.2879$ and kurtosis $Q = 0.1995$. These values agree well with the available numerical estimations.

PACS Nos. 81.15.Aa, 68.35.Fx, 64.60.Ht, 05.10.Cc

Keywords: Kinetic roughening (Theory), Self-affine roughness (Theory), Dynamical processes (Theory), Stochastic processes (Theory).

1. Introduction

The scale invariant growth of a two dimensional surface is a subject of great significance in nonequilibrium statistical mechanics. This is due to its wide range of applicability in addition to its theoretical complexity [1, 2, 3, 4, 5]. It has almost been three decades that Kardar, Parisi, and Zhang [6] proposed a generic equation for surface growth, namely,

$$\frac{\partial h}{\partial t} = \nu_0 \nabla^2 h + \frac{\lambda_0}{2}(\nabla h)^2 + \eta, \tag{1}$$

known as the KPZ equation, where $h(\mathbf{x}, t)$ is the fluctuating height field and ν_0 is the surface tension. The surface grows due to aggregation of particles, modeled by the stochastic noise term $\eta(\mathbf{x}, t)$, which is considered to be Gaussian of zero average with the correlation

$$\langle \eta(\mathbf{x}, t)\eta(\mathbf{x}', t')\rangle = 2D_0\delta^d(\mathbf{x} - \mathbf{x}')\delta(t - t'), \tag{2}$$

where D_0 is referred to as the deposition noise strength and d is the dimension of the substrate.

The KPZ equation in one dimension plays an important role in the application domain. The $(1 + 1)$-dimensional KPZ equation has a semantic relation to a variety of systems. For example, directed polymers in random media (DPRM) [7, 8], vorticity free fluid velocity described by the Burgers equation [9], the stochastic heat equation (SHE) [10], and even sequence alignments in proteins and genes [11, 12], growth phenomena in bacteria colonies [13, 14], turbulent liquid crystals (TLC) [15, 16], slow combustion of a sheet of paper [17, 18, 19], etc., exhibit the same scaling exponents as the $(1 + 1)$-dimensional KPZ equation.

The KPZ equation has been analyzed through renormalization group [20, 21], mode coupling calculation [22, 23, 24], and numerical simulations [25, 26, 27]. Moreover, the scaling functions [28], as well as scaling exponents and the probability distribution function have been studied through finite temperature DPRM in $(1+1)$ dimensions [29] and zero temperature DPRM in $(1 + 1)$ and $(2 + 1)$ dimensions [30].

A considerable amount of understanding of the probability distribution function and its dependence on the initial conditions (namely flat, curved, and stationary) has been achieved through the study of various analytical [31, 32], numerical [33] and experimental [15, 16, 34] methods for different systems that are governed by the $(1+1)$-dimensional KPZ type dynamics. The evolution of a growing surface from a flat initial condition to the stationary state has been studied [35] both numerically (PNG) and experimentally (TLC). The corresponding crossover function is established as universal [36] by considering DPRM, stochastic heat equation (SHE) and growth models which share the universality class of the $(1 + 1)$-dimensional KPZ dynamics.

There exists no exact solution for the $(2 + 1)$-dimensional KPZ equation, which represents a wide variety of surface growth phenomena in real life. Recently the $(2 + 1)$-dimensional KPZ has been realized as an important problem where the higher

dimensional analogs of TW GOE, TW GUE and Baik-Rains distribution have been investigated [10, 37]. Kim et al. [30] studied the minimum energy distribution of directed polymer in random potential with Gaussian distribution up to $(3+1)$ dimensions and obtained non-Gaussian distribution in those dimensions. Halpin-Healy and Takeuchi [38], throughly explored the statistics of the higher dimensional DPRM that yield non-zero skewness and kurtosis values. Alves et al. [39] studied the higher dimensional KPZ height distributions via the RSOS model for flat initial condition and found the distributions to be non-Gaussian.

There have been a large number of numerical works on the $(2+1)$-dimensional KPZ type growth. For instance, the study of the RSOS model by Kim and Kosterlitz [25] leads to estimation of the scaling exponents that agree with their proposed relations $z = 2(d+2)/(d+3)$ and $\beta = 1/(d+2)$ for spatial dimensions $d \leq 4$. Kondev et al. [40] developed an approach wherein properties of scaling of loops of constant height are analyzed to conclude upon geometrical and roughness exponents. They obtained the roughness exponent $\chi = 0.38 \pm 0.08$ via nonlinear estimation. Quite a few growth models having a great deal of diversity, all of which belonging to the $(2+1)$-dimensional KPZ universality class, have been studied [37] for the morphology and statistics in the transient regime. The studied RSOS model, Euler integration of the KPZ equation and the mapping of the KPZ equation to a driven dimer model lead to roughness exponent $\chi = 0.383$, 0.388 and 0.375, respectively. On the other hand, for the stationary state, $\beta = 0.241 \pm 0.001$ [10] and thereby via the well known KPZ scaling relation $\chi(1+1/\beta) = 2$ the roughness exponent is obtained as $\chi = 0.387$–0.390. Kelling and Odor [41] performed a simulation considering a huge size up to $2^{17} \times 2^{17}$ and estimated the scaling exponents $\chi = 0.393 \pm 0.004$ and $\beta = 0.2415$ where the growth exponent of the simulation is higher than $\beta = 0.221$ [42] and $\beta = 0.229$ [43]. Considering a potts-Spin representation via a multisite-coding with 11520^2 sites, Forrest and Tang [26] estimated $\chi = 0.385 \pm 0.005$. An effort via a Monte-Carlo simulation of the hypercube-stacking model of Tang et al. [44] yields the growth exponent $\beta = 0.240 \pm 0.001$. A numerically discretized RSOS model, studied by Marinari et al. [45] by means of multi-surface coding, yields $\chi = 0.393 \pm 0.003$ and $\beta = 0.244 \pm 0.003$. Odor et al. [46] found $\chi = 0.395 \pm 0.005$ by mapping the driven lattice gases of d-dimers model onto the KPZ problem.

Theoretical calculation of χ in two and higher dimensions has been a challenging work. Analytical approaches such as the perturbative RG [6, 20, 47, 21] and nonperturbative approaches, such as mode coupling [22, 48, 24, 49] and self-consistent expansion [50] are incapable of giving any conclusive scaling exponents as well as universality in $d = 2$ dimension. Lässig [51] employed an operator product expansion and obtained $\chi = 2/5$ and $z = 8/5$. A mode coupling calculation of Colaiori and Moore [52] suggested the dynamic exponent $z = 1.62$ and roughness exponent $\chi = 0.38$. A nonperturbative field theoretic RG has been employed by Kloss [53] in the stationary state and obtained roughness exponent $\chi \simeq 0.373$ via amplitude ratio of temporal and spatial correlation [54].

There have been experiments that mimic the $(2 + 1)$-dimensional KPZ scaling and the distribution of height fluctuations. Growth of oligmer thin film due to vapor deposition on a silicon substrate [55] yields the roughness and growth exponents as $\chi = 0.45 \pm 0.04$ and $\beta = 0.28 \pm 0.05$. For the same system, the measured value of skewness $S = 0.23$ [56] in the transient regime indicates that the growth is in the $(2 + 1)$-dimensional KPZ universality class. It is interesting to note that Almeida et al. [57] studied the height fluctuations on a polycrystalline CdTe/Si(100) sample and measured $\beta = 0.27 \pm 0.04$.

From the knowledge of geometry dependent subclasses in $(1 + 1)$ dimensions, it is well known that the scaling exponents are not sufficient to understand the KPZ universality class. For the identification of the universality class, information about the whole distribution function is essential. Moreover, it has been suggested that the measurements of moments are more stable and accurate [4] than the scaling exponents.

Marinari et al. [45] estimated higher order moments through multi-surface coding in different dimensions. From their reported moments in 2D, the skewness and kurtosis can be calculated as $|S| \sim 0.266$ and $Q \sim 0.121$, respectively. Recently, two authors of the same group, Pagnani and Parisi [58] refined the study of $(2 + 1)$-dimensional KPZ-type growth in the steady state and estimated two sets of best-fit results, namely, FIT-I and FIT-II for roughness exponent, skewness and kurtosis values. They found roughness exponent $\chi = 0.3893 \pm 0.0006$ (FIT-I), $\chi = 0.3869 \pm 0.0004$ (FIT-II), skewness $|S| = 0.2669 \pm 0.0004$ (FIT-I), $|S| = 0.2657 \pm 0.0004$ (FIT-II) and kurtosis $Q = 0.146 \pm 0.002$(FIT-I), $Q = 0.145 \pm 0.001$ (FIT-II). Chin and den Nijs [59] have

performed a numerical study of the $(2+1)$-dimensional KPZ equation in the stationary state and obtained the roughness exponent $\chi \approx 0.38$ considering finite size scaling. They concluded that the third moment is more stable and more sensitive (than the roughness exponent) so that it is more suitable to determine and verify the universality class. They found skewness $|S| = 0.27$ and excess kurtosis $Q = 0.15$ which are the same as those in Kim-Kosterlitz (KK) and BCSOS models, thus identifying them to belong to the universality class of the $(2+1)$-dimensional KPZ dynamics.

Halpin-Healy [10] has reported the value of average skewness ($S = 0.244$) and kurtosis ($Q = 0.177$) for three models namely, RSOS, $g5_1$ DPRM and KPZ Euler. In the literature, the roughness and dynamic exponents ($\chi \approx 0.39$, $z \approx 1.61$) have been estimated from a considerable amount of numerical effort. For the purpose of calculating the skewness and kurtosis in $(2+1)$ dimensions, we take $\chi = 9/23$ (and $z = 37/23$, satisfying $\chi + z = 2$) as the sole input. The advantage of taking χ as a rational number is to avoid uncontrollable truncation errors in the subsequent exponents occuring in the calculations. We thus write the renormalized surface tension and noise amplitude as

$$\nu(k) = A\ k^{-9/23} \tag{3}$$

and

$$D(k) = B\ k^{-27/23} \tag{4}$$

where A and B are scale independent constants. The noise correlation in the Fourier space is written as

$$\langle \eta(\mathbf{k},\omega)\eta(\mathbf{k}',\omega')\rangle = 2D_0(2\pi)^d\delta^d(\mathbf{k}+\mathbf{k}')(2\pi)\delta(\omega+\omega'). \tag{5}$$

Although the scaling exponents and universality class of $(1+1)$-dimensional KPZ have been studied extensively, there are few numerical estimations of moments in the (2+1)-dimensional case, whereas analytical treatments are extremely rare. In this paper, we calculate the higher order statistical moments of height fluctuation of the $(2+1)$-dimensional flat KPZ equation in the stationary state. This is achieved by calculating the cumulants up to the fourth order by employing a perturbation scheme to obtain the connected loop diagrams.

This paper is organized in the following way. Section II and Section III present the calculations of the third and fourth cumulants, respectively. In Section IV, we calculate

the second cumulant. Skewness and kurtosis values are obtained from the calculated cumulants in Section V. Finally discussions and conclusions are given in Section VI.

2. The Third Cumulant

Fourier transform of the KPZ equation (Eq. 1) is written as

$$(-i\omega+\nu_0 k^2)h(\mathbf{k},\omega) = \eta(\mathbf{k},\omega) - \frac{\lambda_0}{2}\int\!\!\int \frac{d^d\mathbf{q}d\Omega}{(2\pi)^{d+1}}[\mathbf{q}\cdot(\mathbf{k}-\mathbf{q})]h(\mathbf{q},\Omega)h(\mathbf{k}-\mathbf{q},\omega-\Omega), \quad (6)$$

which will be used for perturbation calculations of cumulants.

The third cumuant $\langle h^3(\mathbf{x},t)\rangle_c$ can be expressed in the Fourier space as

$$W_3 = \langle h^3(\mathbf{x},t)\rangle_c = \int \frac{d^dk_1\,d\omega_1}{(2\pi)^{d+1}}\int \frac{d^dk_2\,d\omega_2}{(2\pi)^{d+1}}\int \frac{d^dk_3\;d\omega_3}{(2\pi)^{d+1}}$$
$$\langle h(\mathbf{k}_1,\omega_1)\,h(\mathbf{k}_2,\omega_2)\,h(\mathbf{k}_3,\omega_3)\rangle_c\; e^{i(\mathbf{k}_1+\mathbf{k}_2+\mathbf{k}_3)\cdot\mathbf{x}}\, e^{-i(\omega_1+\omega_2+\omega_3)t} \quad (7)$$

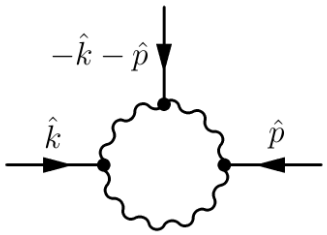

Figure 1. Feynman diagram corresponding to the third cumulant where a wiggly line represents correlation and solid line response.

The third cumulant in Eq. 7 is constructed by using Eq. 6 in a perturbative framework. We follow the diagrammatic approach and obtain a one-loop diagram which contributes to $\langle h^3(\mathbf{x},t)\rangle_c$ as shown in Fig. 1. Consequently, $\langle h^3(\mathbf{x},t)\rangle_c$ is written as

$$\langle h^3(\mathbf{x},t)\rangle_c = \int \frac{d^{d+1}\hat{k}_1}{(2\pi)^{d+1}}\int \frac{d^{d+1}\hat{k}_2}{(2\pi)^{d+1}}\,G(\hat{k}_1)\,G(\hat{k}_2)\,L_3(\hat{k}_1;\hat{k}_2)\,G(-\hat{k}_1-\hat{k}_2) \quad (8)$$

where $L_3(\hat{k}_1;\hat{k}_2)$ indicates the amputated loop (excluding the external legs) and $\hat{k}_1$ stands for $(\mathbf{k}_1,\omega_1)$. We first consider bare value of the loop integral [60] which is expressed as

$$L_3^{(0)}(\mathbf{k}_1,\omega_1;\mathbf{k}_2,\omega_2) = 8\left(\frac{-\lambda_0}{2}\right)^3\int \frac{d^dq\,d\Omega}{(2\pi)^{d+1}}\,[(\mathbf{q}-\mathbf{k}_1)\cdot(\mathbf{k}_2+\mathbf{k}_1-\mathbf{q})]\,[\mathbf{q}\cdot(\mathbf{k}_1-\mathbf{q})]$$
$$[-\mathbf{q}\cdot(\mathbf{q}-\mathbf{k}_2-\mathbf{k}_1)]\,Q_0(\mathbf{q},\Omega)\,Q_0(\mathbf{k}_1-\mathbf{q},\omega_1-\Omega)\,Q_0(\mathbf{k}_1+\mathbf{k}_2-\mathbf{q},\omega_1+\omega_2-\Omega) \quad (9)$$

Frequency and momentum integrations are performed in Eq. 9 in the limit of zero external momenta and frequencies. This gives the leading order contribution in an expansion when the external momenta and frequencies are small with respect to internal ones in the loop integral. The momentum is integrated in the thin shell $\Lambda_0 e^{-r} \leq q \leq \Lambda_0$, yielding

$$L_3^<(r) = \frac{3}{2} K_d \frac{\lambda_0^3 D_0^3}{\nu_0^5 \Lambda_0^{4-d}} \frac{e^{(4-d)r} - 1}{4-d}. \tag{10}$$

where $K_d = S_d/(2\pi)^d$ with S_d the surface area of unit sphere embedded in a d-dimensional space. Assuming that shell elimination is performed in recursive steps [61], we obtain a differential equation for the scale dependent loop as

$$\frac{dL_3}{dr} = \frac{3}{2} K_d \frac{\lambda_0^3 D^3(r)}{\nu^5(r) \Lambda^{4-d}(r)} \tag{11}$$

where $\Lambda(r) = \Lambda_0 e^{-r}$. Using the scaling relations Eq. 3 and 4, and identifying k as $\Lambda_0 e^{-r}$, we integrate Eq. 11 over r, and obtain

$$L_3(r) = \lambda_0^3 \frac{69}{328\pi} \left(\frac{B^3}{A^5} \right) \Lambda_0^{-82/23} e^{82r/23} \tag{12}$$

for $d = 2$. Since $L_3(\hat{k}_1; \hat{k}_2)$ appearing in Eq. 8 represents the (renormalized) loop diagram, its value is determined by the independent momenta $\hat{k}_1$ and $\hat{k}_2$ that flow along two internal lines belonging to the loop. Moreover, $L_3(\hat{k}_1; \hat{k}_2)$ should be symmetric with respect to interchange of momenta $\hat{k}_1$ and $\hat{k}_2$ because the right hand expression in Eq. (8) is expected to be symmetric with respect to the same momentum exchange. Consequently, we construct the momentum dependence in $L_3(\hat{k}_1; \hat{k}_2)$ by considering $\Lambda_0 e^{-r}$ in Eq. (8) as $k_1^{1/2} k_2^{1/2}$. To obtain the dependence on the corresponding external frequencies ω_1 and ω_2, we identify $(\Lambda_0 e^{-r})^{-41/23}$ as $k_i^{-41/23} f_1\left(\frac{\omega_i}{k_i^z}\right)$ where $f_1(.)$ is a dimensionless scaling function given by

$$k_i^{-41/23} f_1\left(\frac{\omega_i}{k_i^z}\right) = k_i^{143/23} \nu^4(k_1) |G(k_i, \omega_i)|^4 \tag{13}$$

with $i = 1, 2$. We thus write

$$L_3(\hat{k}_1; \hat{k}_2) = \lambda_0^3 \frac{69}{328\pi} \left(\frac{B^3}{A^5} \right) k_1^{143/23} k_2^{143/23} \nu^4(k_1) \nu^4(k_2) |G(\mathbf{k}_1, \omega_1)|^4 |G(\mathbf{k}_2, \omega_2)|^4. \tag{14}$$

Using the expression from Eq. 14 in Eq. 8, we obtain

$$\langle h^3(\mathbf{x}, t) \rangle_c = \lambda_0^3 \frac{69}{328\pi} A^3 B^3 \int \frac{d^{d+1}\hat{k}_1}{(2\pi)^{d+1}} \int \frac{d^{d+1}\hat{k}_2}{(2\pi)^{d+1}} k_1^{107/23} k_2^{107/23} |G(\hat{k}_1)|^4 |G(\hat{k}_2)|^4 G(\hat{k}_1) G(\hat{k}_2)$$

$$G(-\hat{k}_1 - \hat{k}_2) \tag{15}$$

We perform the frequency integrations over ω and ω', leading to

$$\langle h^3(\mathbf{x},t)\rangle_c = \lambda_0^3\left(\frac{B}{A^2}\right)^3 \frac{69}{328\pi}\int\frac{d^2k_1}{(2\pi)^2}\int\frac{d^2k_2}{(2\pi)^2}F(\mathbf{k}_1,\mathbf{k}_2) \tag{16}$$

The algebric form of the function $F(\mathbf{k}_1,\mathbf{k}_2)$ is given in Appendix. We perform the integrations in Eq. 16 in cartesian coordinates. The function $F(\mathbf{k}_1,\mathbf{k}_2)$ is symmetric with respect to interchange of $\mathbf{k}_1$ and $\mathbf{k}_2$. Consequently, we can write

$$I = \int d^2k_1\int d^2k_2 F(\mathbf{k}_1,\mathbf{k}_2) = 4[I_1(\mu)+2I_2(\mu)+I_3(\mu)] \tag{17}$$

where

$$I_1(\mu) = \int_0^\infty dk_{1x}\int_0^\infty dk_{2x}\int_\mu^\infty dk_{1y}\int_\mu^\infty dk_{2y}F(k_{1x},k_{1y},k_{2x},k_{2y}), \tag{18}$$

$$I_2(\mu) = \int_0^\infty dk_{1x}\int_0^\infty dk_{2x}\int_\mu^\infty dk_{1y}\int_\mu^\infty dk_{2y}F(k_{1x},-k_{1y},k_{2x},k_{2y}), \tag{19}$$

and

$$I_3(\mu) = \int_0^\infty dk_{1x}\int_0^\infty dk_{2y}\int_\mu^\infty dk_{2x}\int_\mu^\infty dk_{1y}F(-k_{1x},-k_{1y},k_{2x},k_{2y}) \tag{20}$$

where we have introduced an infrared cutoff μ because these integrals diverges at the lower limit. We perform numerical integrations of these functions over k_{1x}, k_{1y}, k_{2x} and k_{2y}, leading to the values

$$I_1(\mu) = 0.032196\ \mu^{-27/23}, \tag{21}$$

$$I_2(\mu) = 0.062963\ \mu^{-27/23}, \tag{22}$$

$$I_3(\mu) = 0.0043277\ \mu^{-27/23}, \tag{23}$$

for very small values of μ close to zero. The value of the third cumulant coming from Eq. 16, in terms of these integration values, is given by

$$\langle h^3(\mathbf{x},t)\rangle_c = \left(\frac{\lambda_0 B}{A^2}\right)^3 \frac{69}{328\pi}\frac{1}{4\pi^4}\left[I_1(\mu)+2I_2(\mu)+I_3(\mu)\right]. \tag{24}$$

3. The Fourth Cumulant

The fourth order cumulant, written in Fourier space, assumes the form

$$\langle h^4(\mathbf{x},t)\rangle_c = \int\frac{d^{d+1}\hat{k}_1}{(2\pi)^{d+1}}\int\frac{d^{d+1}\hat{k}_2}{(2\pi)^{d+1}}\int\frac{d^{d+1}\hat{k}_3}{(2\pi)^{d+1}}\int\frac{d^{d+1}\hat{k}_4}{(2\pi)^{d+1}}$$
$$\langle h(\hat{k}_1)h(\hat{k}_2)h(\hat{k}_3)h(\hat{k}_4)\rangle_c\, e^{i(\hat{k}_1+\hat{k}_2+\hat{k}_3+\hat{k}_4)\cdot\hat{x}}. \tag{25}$$

Following the diagrammatic approach, we obtain a connected loop diagram for the fourth order cumulant in Fourier space occurring in the integrand. The corresponding loop diagram is shown in Fig. 2, which suggests the expression

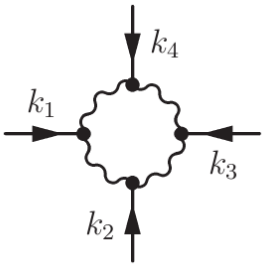

Figure 2. Feynman diagram corresponding to the fourth cumulant where a wiggly line represents correlation and solid line response.

$$\langle h^4(\mathbf{x},t)\rangle_c = \int \frac{d^{d+1}\hat{k}_1}{(2\pi)^{d+1}} \int \frac{d^{d+1}\hat{k}_2}{(2\pi)^{d+1}} \int \frac{d^{d+1}\hat{k}_3}{(2\pi)^{d+1}}\, G(\hat{k}_1)\, G(\hat{k}_2)\, G(\hat{k}_3)$$
$$L_4(\hat{k}_1;\hat{k}_2;\hat{k}_3)\, G(-\hat{k}_1-\hat{k}_2-\hat{k}_3), \tag{26}$$

where $L_4(\hat{k}_1;\hat{k}_2;\hat{k}_3)$ is the contribution coming from the renormalized amputated loop (without the external legs) and $G(\hat{k}_i)$ are the renormalized propagators.

The unrenormalized expression for the amputated loop, in $(d+1)$ dimensions, corresponding to the fourth order cumulant is expressed as [62]

$$L_4^{(0)}(\hat{k}_1;\hat{k}_2;\hat{k}_3) = 16\left(-\frac{\lambda_0}{2}\right)^4 (2D_0)^4 \int \frac{d^{d+1}\hat{q}}{(2\pi)^{d+1}} [\mathbf{q}\cdot(\mathbf{q}-\mathbf{k}_1)][\mathbf{q}\cdot(\mathbf{k}_2+\mathbf{q})]$$
$$[(\mathbf{q}+\mathbf{k}_2)\cdot(\mathbf{k}_3+\mathbf{k}_2+\mathbf{q})][(\mathbf{q}-\mathbf{k}_1)\cdot(\mathbf{q}+\mathbf{k}_2+\mathbf{k}_3)] G_0(\hat{q})$$
$$G_0(-\hat{q}+\hat{k}_1) G_0(-\hat{q}) G_0(\hat{q}+\hat{k}_2) G_0(-\hat{q}-\hat{k}_2) G_0(\hat{q}+\hat{k}_3+\hat{k}_2)$$
$$G_0(\hat{q}-\hat{k}_1) G_0(-\hat{q}-\hat{k}_2-\hat{k}_3), \tag{27}$$

where the suffix 0 signifies unrenormalized quantities. Carrying out the frequency and momentum integration in Eq. 27, we obtain the following expression on elimination of modes from the shell $\Lambda(r) \le q \le \Lambda_0$.

$$L_4^{<}(r) = \frac{5}{2} K_d \frac{\lambda_0^4 D_0^4}{\nu_0^7 \Lambda_0^{6-d}} \frac{e^{(6-d)r}-1}{d-6} \tag{28}$$

Assuming that shell elimination is performed in recursive steps, we obtain

$$\frac{dL_4}{dr} = \frac{5}{2} K_d \frac{\lambda_0^4 D^4(r)}{\nu^7(r)\Lambda^{6-d}(r)} \tag{29}$$

Employing Eq. 3 and 4 with k identified as $\Lambda_0 e^{-r}$ and integrating Eq. 29 over r for $d = 2$ substrate dimensions, we obtain

$$L_4(r) = \frac{115}{548\pi} \left[\frac{\lambda_0^4 D^4(r)}{\nu^7(r)\Lambda^4(r)} \right]. \tag{30}$$

Since the loop $L_4(\hat{k}_1; \hat{k}_2; \hat{k}_3)$ depends on the three external momenta k_1, k_2 and k_3, the expression for $L_4(\hat{k}_1; \hat{k}_2; \hat{k}_3)$ appearing in Eq. 26 is expected to be symmetric with respect to interchange of $\hat{k_1}$, $\hat{k_2}$ and $\hat{k_3}$. Thus the momentum dependence is constructed by considering $\Lambda_0 e^{-r}$ in Eq. 30 as $k_1^{1/3} k_2^{1/3} k_3^{1/3}$. To obtain the dependence on external frequencies ω_1, ω_2 and ω_3, we identify $(\Lambda_0 e^{-r})^{-137/69}$ as $k_j^{-137/69} f_2\left(\frac{\omega_j}{k_j^z}\right)$ where $f_2(.)$ is a dimensionless scaling function. The form of the scaling function is introduced as

$$k_j^{-137/69} f_2\left(\frac{\omega_j}{k_j^z}\right) = k_j^{415/69} \nu^4(k_j) |G(k_j, \omega_j)|^4 \tag{31}$$

where $\hat{k}_j$ represents $\hat{k}_1$ or $\hat{k}_2$ or $\hat{k}_3$. Employing this scaling relation, the renormalized loop in Fig. 3 assumes the form

$$L_4(\hat{k}_1; \hat{k}_2; \hat{k}_3) = \lambda_0^4 \left(\frac{B^4}{A^7}\right) \frac{115}{548\pi} \prod_{j=1}^{3} k_j^{415/69} \nu^4(k_j) |G(\hat{k}_j)|^4 \tag{32}$$

Using the expression from Eq. 32 in Eq. 26, we obtain

$$\begin{aligned} \langle h^4(\mathbf{x}, t) \rangle_c &= \lambda_0^4 A^5 B^4 \frac{115}{548\pi} \int \frac{d^{d+1}\hat{k}_1}{(2\pi)^{d+1}} \int \frac{d^{d+1}\hat{k}_2}{(2\pi)^{d+1}} \int \frac{d^{d+1}\hat{k}_3}{(2\pi)^{d+1}} G(-\hat{k}_1 - \hat{k}_2 - \hat{k}_3) \\ &\quad \prod_{j=1}^{3} k_j^{307/69} |G(\hat{k}_j)|^4 G(\hat{k}_j) \end{aligned} \tag{33}$$

where the response function involves the renormalized surface tension $\nu(\mathbf{k})$. Carrying out the frequency integrations yields

$$\langle h^4(\mathbf{x}, t) \rangle_c = \left(\frac{\lambda_0 B}{A^2}\right)^4 \frac{115}{548\pi} \int \frac{d^2 k_1}{(2\pi)^2} \int \frac{d^2 k_2}{(2\pi)^2} \int \frac{d^2 k_3}{(2\pi)^2} T(\mathbf{k}_1, \mathbf{k}_2, \mathbf{k}_3) \tag{34}$$

where the form of $T(\mathbf{k}_1, \mathbf{k}_2, \mathbf{k}_3)$ is given in Appendix. For brevity in notations, henceforth we rename the momenta $\mathbf{k}_1$, $\mathbf{k}_2$ and $\mathbf{k}_3$ as $\mathbf{k}$, $\mathbf{p}$ and $\mathbf{q}$. Subsequently, we express the integrations in cartesian coordinates, so that

$$\begin{aligned} \langle h^4(\mathbf{x}, t) \rangle_c = \frac{\lambda_0^4}{(2\pi)^6} \frac{B^4}{A^8} \frac{115}{548\pi} [&\int_{-\infty}^{\infty} dk_x \int_{-\infty}^{\infty} dk_y \int_{-\infty}^{\infty} dp_x \int_{-\infty}^{\infty} dp_y \\ &\int_{-\infty}^{\infty} dq_x \int_{-\infty}^{\infty} dq_y T(k_x, k_y; p_x, p_y; q_x, q_y)] \end{aligned} \tag{35}$$

Due to the symmetry of the integrand in momentum variables, we can break the function as

$$\langle h^4(\mathbf{x},t)\rangle_c = \frac{4}{(2\pi)^6}\left(\frac{\lambda_0 B}{A^2}\right)^4 \frac{115}{548\pi}\int_0^\infty dk_x \int_0^\infty dk_y \int_0^\infty dp_x \int_0^\infty dp_y \int_0^\infty dq_x \int_0^\infty dq_y$$
$$\{T(k_x,k_y;p_x,p_y;q_x,q_y) + 6T(k_x,-k_y;p_x,p_y;q_x,q_y) + 9T(-k_x,-k_y;p_x,p_y;q_x,q_y)\} \quad (36)$$

The momentum dependence causes the integrations to diverge in the infrared limit. Therefore, we set μ as the lower cutoff of the integrations and express the integration in terms of

$$J_1(\mu) = \int_0^\infty dk_x \int_0^\infty dk_y \int_0^\infty dp_x \int_\mu^\infty dp_y \int_\mu^\infty dq_x \int_\mu^\infty dq_y T(k_x,k_y;p_x,p_y;q_x,q_y), \quad (37)$$

$$J_2(\mu) = \int_0^\infty dk_x \int_0^\infty dk_y \int_0^\infty dp_x \int_\mu^\infty dp_y \int_\mu^\infty dq_x \int_\mu^\infty dq_y T(k_x,-k_y;p_x,p_y;q_x,q_y) \quad (38)$$

and

$$J_3(\mu) = \int_0^\infty dk_x \int_0^\infty dk_y \int_0^\infty dp_x \int_\mu^\infty dp_y \int_\mu^\infty dq_x \int_\mu^\infty dq_y T(-k_x,-k_y;p_x,p_y;q_x,q_y) \quad (39)$$

so that

$$\langle h^4(\mathbf{x},t)\rangle_c = \frac{4}{(2\pi)^6}\left(\frac{\lambda_0 B}{A^2}\right)^4 \frac{115}{548\pi}\left[J_1(\mu) + 6J_2(\mu) + 9J_3(\mu)\right]. \quad (40)$$

Performing the integrations numerically, we obtain

$$J_1(\mu) = 0.0069369\mu^{-36/23}, \quad (41)$$

$$J_2(\mu) = 0.0000151\mu^{-36/23}, \quad (42)$$

and

$$J_3(\mu) = 0.0219628\mu^{-36/23}. \quad (43)$$

We shall employ these numerical values in the next Section while calculating the value of kurtosis.

4. The Second Cumulant

In order to calculate the skewness and kurtosis, we need in addition to the third and fourth, the second cumulant. The first moment, $\langle h(\mathbf{x},t)\rangle$, is zero in the steady state, where the angular brackets denote as ensemble average. The second cumulant is expressed in the Fourier space as

$$W_2 = \langle h^2(\mathbf{x},t)\rangle_c = \int \frac{d^dk d\omega}{(2\pi)^{d+1}} \int \frac{d^dk' d\omega'}{(2\pi)^{d+1}} \langle h(\mathbf{k},\omega)h(\mathbf{k}',\omega')\rangle_c e^{i(\mathbf{k}+\mathbf{k}')\cdot\mathbf{x}} e^{-i(\omega+\omega')t}. \quad (44)$$

where the height-height correlation is given by

$$\langle h(\mathbf{k},\omega)h(\mathbf{k}',\omega')\rangle = Q(\mathbf{k},\omega)(2\pi)^d\delta^d(\mathbf{k}+\mathbf{k}')(2\pi)\delta(\omega+\omega') \tag{45}$$

with $Q(\mathbf{k},\omega)$ the renormalized correlation. Using Eq. (45) in Eq. (44) leads to

$$\langle h^2(\mathbf{x},t)\rangle_c = \int \frac{d^dk\ d\omega}{(2\pi)^{d+1}} Q(\mathbf{k},\omega). \tag{46}$$

The correlation, $Q(\mathbf{k},\omega)$, can be obtained perturbatively using Eqs. (6) and (45). To obtain the leading order contribution to the second cumulant, we consider the one loop diagram shown in Fig.3, that satisfies the expression

$$Q(\mathbf{k},\omega) = G(\mathbf{k},\omega)L_2(\mathbf{k},\omega)G(-\mathbf{k},-\omega) \tag{47}$$

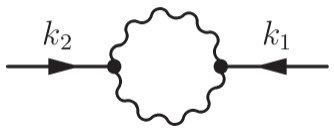

Figure 3. Feynman diagram corresponding to the second cumulant where a wiggly line represents correlation and solid line response.

Equation 47 corresponds to the loop diagram in Fig.3. The unrenormalized amputated loop (excluding the external legs) is expressed as

$$L_2^{(0)}(\mathbf{k},\omega) = 2\left(\frac{-\lambda_0}{2}\right)^2 \int_{\Lambda(r)}^{\Lambda_0} \frac{d^dq}{(2\pi)^d} \int_{-\infty}^{\infty} \frac{d\omega}{(2\pi)} [\mathbf{q}\cdot(\mathbf{k}-\mathbf{q})]^2 |G_0(\hat{\mathbf{q}})|^2 |G_0(\hat{\mathbf{k}}-\hat{\mathbf{q}})|^2 |(2D_0)^2 \tag{48}$$

that contains unrenormalized noise amplitude D_0 and unrenormalized response function $G_0(\mathbf{k},\omega) = [-i\omega+\nu_0k^2]^{-1}$. Carrying out the frequency integration in the whole range and the momentum integration in the shell $\Lambda_0 e^{-r} \le q \le \Lambda_0$, we obtain

$$L_2^<(r) = \frac{\lambda_0^2 D_0^2 K_d}{2\nu_0^3}\left[\frac{\Lambda_0^{d-2} - \Lambda^{d-2}(r)}{(d-2)}\right]. \tag{49}$$

We construct a differential equation for L_2 with respect to the scale parameter r,

$$\frac{dL_2}{dr} = K_d \frac{\lambda_0^2 D^2(r)}{2\nu^3(r)\Lambda^{2-d}(r)} \tag{50}$$

where $\Lambda(r) = \Lambda_0 e^{-r}$. Using the scale dependence from Eqs. 3 and 4, and integrating over r leads to

$$L_2(r) = \frac{23}{108\pi}\left(\frac{\lambda_0^2 B^2}{A^3}\right)(\Lambda_0 e^{-r})^{-27/23} \tag{51}$$

for $d = 2$. We consider the scale dependent parameter $(\Lambda_0 e^{-r})^{-27/23}$ as $k^{-27/23}\ f\left(\frac{\omega}{k^z}\right)$, where $f\,(.)$ dimensionless scaling function and z is the dynamic exponent. Thus $L_2(\mathbf{k};\omega)$ is expressed as

$$L_2(\mathbf{k};\omega) = \frac{23}{108\pi}\left(\frac{\lambda_0^2\ B^2}{A^3}\right) k^{-27/23}\ f\left(\frac{\omega}{k^z}\right). \tag{52}$$

As before, we write

$$k^{-27/23} f\left(\frac{\omega}{k^z}\right) = k^{3861/943}\nu^{108/41}(k)|G(\mathbf{k},\omega)|^{108/41} \tag{53}$$

so that $L_2(\mathbf{k};\omega)$ becomes

$$L_2(\mathbf{k};\omega) = \frac{23}{108\pi}\left(\frac{\lambda_0^2\ B^2}{A^3}\right) k^{3861/943}\nu^{108/41}(k)\ |G(\mathbf{k},\omega)|^{108/41} \tag{54}$$

From Eqs. 46 and 47, we have

$$\langle h^2(\mathbf{x},t)\rangle_c = \int \frac{d^dk}{(2\pi)^d}\int\frac{d\omega}{(2\pi)}|G(\mathbf{k},\omega)|^2 L_2(\mathbf{k};\omega) \tag{55}$$

where we substitute the expression for L_2 given by Eq. 54, so that

$$\langle h^2(\mathbf{x},t)\rangle_c = \frac{23}{108\pi}\left(\frac{\lambda_0^2 B^2}{A^3}\right) A^{108/41}\int\frac{d^2k}{(2\pi)^2}k^{2889/943}\int\frac{d\omega}{(2\pi)}\frac{1}{[\omega^2+\nu^2(k)k^4]^{95/41}}, \tag{56}$$

where the surface tension $\nu(k)$ in the denominator is renormalized. Performing the frequency integration and expressing the momentum integration in cartesian coordinates, we obtain

$$\langle h^2(\mathbf{x},t)\rangle_c = \frac{23}{108\pi}\left(\frac{\lambda_0 B}{A^2}\right)^2\left(\frac{\Gamma\left(\frac{149}{82}\right)}{2\sqrt{\pi}\ \Gamma\left(\frac{95}{41}\right)}\right)\left[\frac{4}{4\pi^2}\int_0^\infty dk_x\int_0^\infty dk_y\frac{1}{[k_x^2+k_y^2]^{32/23}}\right]. \tag{57}$$

The factor of 4 appears because the integrand is an even function of k_x and k_y. Moreover, the integration in the Eq. 57 is symmetric with respect to interchange of k_x and k_y. We first do the momentum integration over k_x with limits, $0 \le k_x \le \infty$ yielding

$$\langle h^2(\mathbf{x},t)\rangle_c = \frac{23}{108\pi^3}\left(\frac{\lambda_0 B}{A^2}\right)^2\left(\frac{\Gamma\left(\frac{149}{82}\right)}{2\sqrt{\pi}\ \Gamma\left(\frac{95}{41}\right)}\right)\left(\frac{\sqrt{\pi}}{2}\frac{\Gamma\left(\frac{41}{46}\right)}{\Gamma\left(\frac{32}{23}\right)}\right)\left[\int_\mu^\infty dk_y k_y^{-41/23}\right] \tag{58}$$

We have introduced an infrared cutoff μ as the integral on k_y diverges at the lower limit. We thus obtain by integration

$$\langle h^2(\mathbf{x},t)\rangle_c = [0.211105\times 10^{-2}]\ \left(\frac{\lambda_0 B}{A^2}\right)^2\frac{1}{\mu^{18/23}} \tag{59}$$

where we have used $\Gamma\left(\frac{149}{82}\right) = 0.936026$, $\Gamma\left(\frac{95}{41}\right) = 1.178818$, $\Gamma\left(\frac{41}{46}\right) = 1.075746$ and $\Gamma\left(\frac{32}{23}\right) = 0.887772$. This is the second cumulant of the height fluctuations in the stationary state of the $2+1$ KPZ equation.

5. Skewness and Kurtosis

In this section, we calculate the skewness and kurtosis of the height fluctuations obeying the $(2+1)$-dimensional KPZ equation in the stationary state. For this purpose, we use the values of the second, third and fourth order moments evaluated above. The n th moments is expressed as

$$W_n = \langle [h(\mathbf{x},t) - \langle h \rangle]^n \rangle \tag{60}$$

which is related to the system size as $W_n \sim L^{n\chi}$, where L is the size of the system. Substituting $n = 3$ and 4 in Eq. 60, we obtain the expressions

$$W_2 = \langle h^2 \rangle - \langle h \rangle^2, \tag{61}$$

$$W_3 = \langle h^3 \rangle - 3\langle h \rangle \langle h^2 \rangle + 2\langle h \rangle^3 \tag{62}$$

$$W_4 = \langle h^4 \rangle - 4\langle h \rangle \langle h^3 \rangle + 6\langle h^2 \rangle \langle h \rangle^2 - 3\langle h^2 \rangle^2. \tag{63}$$

The moments and cumulants are related as

$$\begin{aligned}
\langle h \rangle &= \langle h \rangle_c \\
\langle h^2 \rangle &= \langle h^2 \rangle_c + \langle h \rangle_c^2 \\
\langle h^3 \rangle &= \langle h^3 \rangle_c + 3\langle h \rangle_c \langle h^2 \rangle_c + \langle h \rangle_c^3 \\
\langle h^4 \rangle &= \langle h^4 \rangle_c + 4\langle h \rangle_c \langle h^3 \rangle_c + 3\langle h^2 \rangle_c^2 + 6\langle h \rangle_c^2 \langle h^2 \rangle_c + \langle h \rangle_c^4
\end{aligned} \tag{64}$$

These higher order moments determine the values of skewness and kurtosis. Taking ensemble average on both sides of Eq. (6), we find that both terms on the right hand side vanish because the noise is Gaussian and the second term yields a Dirac delta function $\delta^d(\mathbf{k})$ upon using Eq. (45). Finiteness of the substrate (although it is assumed to be large) implies that $\langle h \rangle = 0$. Thus, skewness and kurtosis may be expressed as

$$S = \frac{\langle h^3 \rangle}{\langle h^2 \rangle^{3/2}} = \frac{\langle h^3 \rangle_c}{\langle h^2 \rangle_c^{3/2}} \tag{65}$$

and

$$Q = \frac{\langle h^4 \rangle}{\langle h^2 \rangle^2} - 3 = \frac{\langle h^4 \rangle_c}{\langle h^2 \rangle_c^2} \tag{66}$$

where the suffix c indicates the cumulants that correspond to connected diagramms in the perturbative expansion. Skewness S measures the asymmetry of the distribution

function with respect to the Gaussian. A positive (negative) value of skewness is obtained when the distribution has a longer tail on the right (left) side. The Q value indicates sharpness with respect to the Gaussian distribution. A positive (negative) value of Q signifies a sharper (flatter) distribution than the Gaussian.

We obtain the skewness and kurtosis employing the above definitions. Using the numerically evaluated integrations of $I_1(\mu)$, $I_2(\mu)$ and $I_3(\mu)$ in Eq. 24, we obtain

$$\langle h^3(\mathbf{x},t)\rangle_c = [0.027922 \times 10^{-3}] \left(\frac{\lambda_0 B}{A^2}\right)^3 \mu^{-27/23}. \tag{67}$$

Substituting from equations 59 and 67 in Eq. 65, we calculate the skewness of the $(2+1)$-dimensional KPZ height distribution as

$$S = \frac{\langle h^3(\mathbf{x},t)\rangle_c}{\langle h^2(\mathbf{x},t)\rangle_c^{3/2}} = \frac{0.027922}{(0.211105)^{3/2}} = 0.2879. \tag{68}$$

Similarly, we substitute the results of the evaluated numerical integrations $J_1(\mu)$, $J_2(\mu)$ and $J_3(\mu)$ in Eq. 40, obtaining

$$\langle h^4(\mathbf{x},t)\rangle_c = [0.008889 \times 10^{-4}] \left(\frac{\lambda_0 B}{A^2}\right)^4 \mu^{-36/23}. \tag{69}$$

Using Eq. 69 and Eq. 59 in Eq. 66 leads to the kurtosis value as

$$Q = \frac{\langle h^4(\mathbf{x},t)\rangle_c}{\langle h^2(\mathbf{x},t)\rangle_c^2} = \frac{0.008889}{(0.211105)^2} = 0.1995 \tag{70}$$

We note that these values for skewness and kurtosis are obtained for the $(2+1)$-dimensional KPZ dynamics corresponding to the stationary state.

6. Discussion and Conclusion

Our main motivation in this work comes from two facts. First, the growth of a surface on a 2D substrate is a commonly occurring phenomenon in Nature. Second, analytical methodologies to obtain the skewness and kurtosis values directly from the dynamical equation are unavailable in the existing literature. The obtained skewness $S = 0.2879$ and kurtosis $Q = 0.1995$ values are independent of model parameters (ν_0, D_0, and λ_0), scaling coefficients (A and B) and the momentum cutoffs (Λ_0 and μ) in the calculations. The sole input to our calculations is the roughness exponent $\chi = 9/23 = 0.391304$ which is a good approximation to high resolution numerical results.

In this context it may be noted that most analytical approaches have been unsuccessful to obtain the scaling exponents in $(2+1)$ dimensions, apart from the

works of Lässig [51], Tu [49] Colaiori and Moore [52] and Kloss et al.[54], as mentioned earlier. At the same time, a huge amount of numerical approaches suggest the roughness and dynamic exponents to be $\chi \approx 0.39$ and $z \approx 1.61$, respectively.

We employed perturbation theory directly on the KPZ equation to obtain expressions for $L_3^<(r)$, $L_4^<(r)$ and $L_2^<(r)$ that contain the bare parameters ν_0 and D_0. Obtaining these expressions solely depend on the use of perturbation theory and they do not incorporate the renormalization group in the conventional sense. We use these expressions for $L_3^<(r)$, $L_4^<(r)$, and $L_2^<(r)$ to obtain the flow equations for the renormalized quantities $L_3(r)$, $L_4(r)$, and $L_2(r)$ that involve the renormalized quantities $\nu(r)$ and $D(r)$. In this process, we are able to find explicit mathematical relations including the prefactors once the scaling laws for the effective surface tension $\nu(k)$ and the noise amplitude $D(k)$ are assumed (Eqs. (3) and (4)) in consistency with the scaling relation $\chi + z = 2$. We incorporate frequency dependence of these loops by scaling functions that preserve their real valuedness and their correct zero frequency limits. This allows for the calculation of the corresponding cumulants that are found to depend on the infrared cutoff μ as $W_n \sim \mu^{-n\chi}$. This is expected because the cumulants have the semi-extensive property $W_n \sim L^{n\chi}$ in the stationary state where L is the substrate size. Thus the infrared cutoff can be identified as $\mu \sim L^{-1}$. We finally obtain the skewness value $S = 0.2879$ and the kurtosis value $Q = 0.1995$, relevant to the case of (2+1)-dimensional KPZ growth in the stationary state.

It may be noted that it is not possible to incorporate the results of the standard renormalization group analyses that do not yield a strong coupling fixed point and thereby providing no prediction for the value of χ in two dimensions. On the other hand, mode-coupling theories suggest that the upper critical dimension is 3.6, 4 or ∞ [63, 52, 49]. Interestingly, a non-perturbative renormalization group analysis [53] indicated the existence of a stable strong coupling fixed point for $d \leq 2$, whereas for $d > 2$, there exist two basins of attraction containing a Gaussian fixed point and a strong coupling fixed point. The resulting roughness exponent was found to be $\chi = 0.330(8)$ and $\chi = 0.373(1)$ (in two dimensions) in the leading and next to leading order approximations, respectively. The latter result agrees very well with the numerical estimation $\chi \approx 0.39$ that we have used in our calculations. We further note that the values for the amplitudes A and B (that determine the fixed point value $g^* \sim \lambda_0^2 B/A^3$

) are not required in our calculations because they cancel out in the ratios determining S and Q.

It can be seen that the scalings of the renormalized quantities are $\nu(k) \sim k^{-\chi}$ and $D(k) \sim k^{-3\chi+2-d}$ in d dimensions. Consequently, the scalings for the loop functions turn out to be $L_3(k) = C_3\, k^{-4\chi-2d+2}$, $L_4(k) = C_4\, k^{-5\chi-3d+2}$ and $L_2(k) = C_2\, k^{-3\chi-d+2}$. We expect these scaling relations to be correct for any (non-zero) value of χ because they have been obtained on the basis of counting momentum dimensions. These relations suggest that $dL_3/dr = (4\chi + 2d - 2)\, C_3\, \Lambda_0^{-4\chi-2d+2}\, e^{(4\chi+2d-2)r}$, $dL_4/dr = (5\chi + 3d - 2)\, C_4\, \Lambda_0^{-5\chi-3d+2}\, e^{(5\chi+3d-2)r}$ and $dL_2/dr = (3\chi + d - 2)\, C_2\, \Lambda_0^{-3\chi-d+2}\, e^{(3\chi+d-2)r}$. These flow equations for $L_3(r)$, $L_4(r)$ and $L_2(r)$ contain unknown constants C_3, C_4 and C_2 respectively. The use of perturbation theory in our calculations serves to find these flow equations, along with the unknown constants, directly from the KPZ equation. In addition, we see that a good numerical input for χ results in good estimates for skewness and kurtosis values.

All recent numerical simulations in $(2 + 1)$ dimensions suggest that the roughness exponent χ is very close to 0.39 which is close to 9/23 (0.391304). We therefore slightly vary the value of the roughness exponent to $\chi = 19/50$ $(= 0.38)$ and $\chi = 2/5$ $(= 0.40)$ and recalculate the integrals. We find that skewness and kurtosis values undergo shifts by less than 5% from the calculated values given in Eqs. (67) and (69).

The estimated skewness and kurtosis values of Chin and den Nijs [59] via the Kim-Kosterlitz (KK) and BCSOS models are given in Table 1. Although their roughness exponents differed in the two models (KK: $\chi = 2/5$ and BCSOS: $\chi \sim 0.38$), their skewness value ($|S| = 0.27 \pm 0.01$) was the same for both models. Consequently, they concluded that the third moment is more reliable than the roughness exponent for a better identification of the universality class. Their kurtosis value was $Q = 0.15 \pm 0.02$ for both models.

Reis [43] considered the stationary states for etching, ballistic deposition, and body-centered restricted solid-on-solid (BCRSOS) models that suggested the universality of the absolute values of skewness and kurtosis. The best estimates come from etching model which yielded $|S| = 0.26 \pm 0.01$ and $Q = 0.134 \pm 0.015$.

Miranda and Reis [64] used Euler discretization method for numerical integration of the KPZ equation and obtained roughness exponent $0.37 \leq \chi \leq 0.40$. In addition, they

estimated skewness $S = 0.25 \pm 0.01$ and kurtosis $Q = 0.15 \pm 0.1$ by extrapolating data in the limit of large substrate size L. Marinari et al. [45] obtained skewness $S \sim 0.266$ and kurtosis $Q \sim 0.121$ through a numerical RSOS model.

Halpin-Healy [10] considered the $(2+1)$-dimensional numerical models such as $g5_1$ DPRM, RSOS and KPZ Euler in the asymptotic limit of time ($t >> L^z$) and obtained a $(2+1)$-dimensional analog of $(1+1)$-dimensional Baik-Rains distribution from these numerical models. In addition, they calculated the Baik-Rains constant from those numerical models. On the other hand, instead of full probability distribution function only the skewness and kurtosis values have been estimated via the Kim-Kosterlitz (KK), BCSOS models [59], etching model [43], and KPZ Euler discretization approach [64], as displayed in Table-I.

Experiments on vapor deposited oligmer thin film growth [55, 56] yield the roughness and growth exponents $\chi = 0.45 \pm 0.04$ and $\beta = 0.28 \pm 0.05$, and the measured value of skewness $S = 0.23$, suggesting that this growth is in the KPZ universality class. Halpin-Healy and Palasantzas [65] examined two point statistics, in particular, spatial covariance by using the experimental results [55]. In addition, they studied the local squared roughness distribution and extremal height distribution via Euler integration of $(2+1)$ KPZ and compared with the experimental results.

Derrida and Appert [66] (DA) defined a ratio $R_{DA} = S^2/Q$ in $1+1$ dimensions, called the Derrida-Appert ratio [38], and estimated the ratio as $R_{DA} = 0.41517$, which is very close to the estimations from asymmetric simple exclusion principle (ASEP), BD and Brick models in asymptotic time limit, suggesting that R_{DA} is universal for the KPZ dynamics. In these dimensions, R_{DA} is conjectured to be universal via the Derrida-Lebowitz universal scaling function (DLSF) which is independent of any model parameters [67]. Subsequently, Prähofer and Spohn [33] estimated skewness $S = 0.35941$ and kurtosis $Q = 0.28916$ for $(1+1)$-dimensional KPZ height fluctuations in the stationary state and thereby, DA ratio is calculated as $R_{DA} = 0.44673$. Halpin-Healy and Takeuchi [38] studied the higher dimensional numerical models of KPZ class and different geometrical sub-classes namely point-point, point-line and point-plane in the transient regime and found a approximate constant value of R_{DA}. Alves et al. [39] studied the transient state RSOS model starting from the flat initial condition in higher dimensions $d = 3, 4, 5, 6$ and found $S \sim d^{0.46}$ and $Q \sim d^{0.92}$. This appears to suggest

that S^2/Q is independent of d, supporting the greater universality of Derrida-Appert ratio proposed in [38], via their extensive examination of KPZ systems in the transient regime, across dimensions, as well as geometry. Our calculated skewness and kurtosis values yield $R_{DA} = 0.41547$, the normalized values of which is compared with the other stationary value in Table 1.

Table 1. Stationary state values of Skewness and Kurtosis in $(2+1)$ dimensions.

System of study	*Method*	$\lvert S\rvert$	Q	R_{DA}	*Reference*
$g5_1$ DPRM	Numerical	0.240	0.18	0.32	[10]
$2+1$ RSOS	Numerical	0.256	0.18	0.364	[10]
KPZ Euler	Numerical	0.236	0.17	0.328	[10]
KPZ Equation	Numerical	0.25 ± 0.01	0.15 ± 0.1	0.42 ± 0.31	[64]
Etching model	Numerical	0.26 ± 0.01	0.134 ± 0.015	0.50 ± 0.09	[43]
KK and BCSOS	Numerical	0.27 ± 0.01	0.15 ± 0.02	0.49 ± 0.08	[59]
(2+1) RSOS (FIT-I)	Numerical	0.2669 ± 0.0004	0.146 ± 0.002	0.488 ± 0.008	[58]
(2+1) RSOS (FIT-II)	Numerical	0.2657 ± 0.0004	0.145 ± 0.001	0.487 ± 0.005	[58]
Present work	Analytical	0.2879	0.1995	0.4155	Eqs. 68, 70

The universality class of a dynamical system is an important statistical property. In the earlier studies on surface growth, the universality class used to be obtained from only the scaling exponents. In the last two decades, it has been realized that despite the same scaling exponents, the distribution functions can be entirely different due to different initial conditions corresponding to different sub-universality classes. Thus the distribution function contains more statistical information about the system than the scaling exponents. The analytical calculation of the distribution function is hardly possible. To economize on the amount of calculations, one can calculate a few higher order cumulants of the distribution function, the normalized values of which can be used as identifiers of the universality classes.

Appendix

The term $F(\mathbf{k}, \mathbf{p})$ appearing in Eq. 16 is defined as

$$F = (F_1 + F_2 + F_3 + F_4)/R$$

We define $a = 37/23$, $b = 41/23$, and $P = |\mathbf{k}_1 + \mathbf{k}_2|$, so that

$$F_1(\mathbf{k}_1, \mathbf{k}_2) = 33\ k_1^{4a} + 4\ k_1^{3a}(47\ k_2^a + 24\ P^a)$$

$$F_2(\mathbf{k}_1, \mathbf{k}_2) = 3(k_2^a + P^a)^2(11k_2^{2a} + 10k_2^a P^a + 3P^{2a})$$

$$F_3(\mathbf{k}_1, \mathbf{k}_2) = 2k_1^{2a}(203k_2^{2a} + 176k_2^a P^a + 51P^{2a})$$

$$F_4(\mathbf{k}_1, \mathbf{k}_2) = 4k_1^a(47k_2^{3a} + 88k_2^{2a} P^a + 53k_2^a P^{2a} + 12P^{3a})$$

$$R(\mathbf{k}_1, \mathbf{k}_2) = 256k_1^b k_2^b(k_1^a + k_2^a + P^a)^5$$

The function $T(\mathbf{k}, \mathbf{p}, \mathbf{q})$ appearing in Eq. 34 is expressed as

$$T = (T_1 + T_2 + T_3 + T_4 + T_5 + T_6)/S$$

where

$$T_1(\mathbf{k}, \mathbf{p}, \mathbf{q}) = 3\{33k^{6a} + 2k^{5a}(127p^a + 127q^a + 81Q^a)\}$$

$$T_2(\mathbf{k}, \mathbf{p}, \mathbf{q}) = 3[k^{4a}\{815p^{2a} + 815q^{2a} + 986q^a Q^a + 327Q^{2a} + 34p^a(51q^a + 29Q^a)\}]$$

$$T_3(\mathbf{k}, \mathbf{p}, \mathbf{q}) = 3[4k^{3a}\{297p^{3a} + 297q^{3a} + 585q^{2a}Q^a + 375q^a Q^{2a} + 87Q^{3a}$$
$$+ 3p^{2a}(397q^a + 195Q^a) + p^a(1191q^{2a} + 1234q^a Q^a + 375Q^{2a})\}]$$

$$T_4(\mathbf{k}, \mathbf{p}, \mathbf{q}) = 3[(p^a + q^a + Q^a)^2\{(33p^{4a} + 4p^{3a}(47q^a + 24Q^a)$$
$$+ 3(q^a + Q^a)^2(11q^{2a} + 10q^a Q^a + 3Q^{2a}) + 2p^{2a}(203q^{2a} + 176q^a Q^a + 51Q^{2a})$$
$$+ 4p^a(47q^{3a} + 88q^{2a}Q^a + 53q^a Q^{2a} + 12Q^{3a})\}]$$

$$T_5(\mathbf{k},\mathbf{p},\mathbf{q}) = 3[k^{2a}\{815p^{4a} + 12p^{3a}(397q^a + 195Q^a) + (q^a + Q^a)^2$$
$$(815q^{2a} + 710q^aQ^a + 207Q^{2a}) + 2p^{2a}(5277q^{2a} + 4366q^aQ^a + 1221Q^{2a})$$
$$+ 4p^a(1191q^{3a} + 2183q^{2a}Q^a + 1273q^aQ^{2a} + 281Q^{3a})\}]$$

$$T_6(\mathbf{k},\mathbf{p},\mathbf{q}) = 3[2k^a\{127p^{5a} + 17p^{4a}(51q^a + 29Q^a) + (q^a + Q^a)^3(127q^{2a} + 112q^aQ^a + 33Q^{2a})$$
$$+ p^a(q^a + Q^a)^2(867q^{2a} + 734q^aQ^a + 211Q^{2a}) + p^{3a}(2382q^{2a} + 2468q^aQ^a + 750Q^{2a})$$
$$+ p^{2a}(2382q^{3a} + 4366q^{2a}Q^a + 2546q^aQ^{2a} + 562Q^{3a})\}]$$

and

$$S(\mathbf{k},\mathbf{p},\mathbf{q}) = 4096k^{4a}p^{4a}q^{4a}(k^a + p^a + q^a + Q^a)^7$$

where $Q = |\mathbf{k} + \mathbf{p} + \mathbf{q}|$

Acknowledgments

T.S. is thankful to the Ministry of Human Resource Development (MHRD), Government of India, for financial support through a scholarship. M.K.N. is indebted to the Indian Institute of Technology Delhi, and particularly to Prof. Ravisankar and Prof. Senthilkumaran, for hospitality at I.I.T. Delhi.

References

[1] Barabási A-L and Stanley H E 1995 *Fractal Concepts in Surface Growth* (Cambridge: Cambridge University Press)

[2] Krug J 1997 *Adv. Phys.* **46** 139

[3] Halpin-Healy T and Zhang Y-C 1995 *Phys. Rep.* **254** 215

[4] Meakin P 1993 *Phys. Rep.* **235** 189

[5] Family F and Vicsek T 1985 *J. Phys. A: Math. Gen.* **18** L75

[6] Kardar M, Parisi G, and Zhang Y-C 1986 *Phys. Rev. Lett.* **56** 889

[7] M. Kardar and Y.-C. Zhang 1987 Phys. Rev. Lett. **58**, 2087

[8] D. S. Fisher and D. A. Huse 1991 Phys. Rev. B **43**, 10728 .

[9] D. Forster, D. R. Nelson, and M. J. Stephen 1977 Phys. Rev. A **16**, 732

[10] T. Halpin-Healy 2013 Phys. Rev. E **88**, 042118

[11] T. Hwa and M. Lässig 1996 Phys. Rev. Lett. **76**, 2591

[12] T. Hwa 1999 Nature (London) **399**

[13] T. Vicsek, M. Cserz, and V. K. Horvth 1990 Physica A **167**, 315

[14] M. A. C. Huergo, M. A. Pasquale, A. E. Bolzán, A. J. Arvia, and P. H. González, 2010 Phys. Rev. E **82**, 031903

[15] K. A. Takeuchi and M. Sano 2010 Phys. Rev. Lett. **104**, 230601

[16] K. A. Takeuchi, M. Sano, T. Sasamoto, and H. Spohn 2011 Sci. Rep. **1**, 34

[17] J. Maunuksela, M. Myllys, O.-P. Kähkönen, J. Timonen, N. Provatas, M. J. Alava, and T. Ala-Nissila 1997 Phys. Rev. Lett. **79**, 1515

[18] M. Myllys, J. Maunuksela, M. Alava, T. Ala-Nissila, J. Merikoski, and J. Timonen 2001 Phys. Rev. E **64**, 036101

[19] L. Miettinen, M. Myllys, J. Merikoski, and J. Timonen 2005 Eur. Phys. J. B **46**, 55

[20] E. Medina, T. Hwa, M. Kardar, and Y.-C. Zhang 1989 Phys. Rev. A **39**, 3053

[21] E. Frey and U. C. Täuber 1994 Phys. Rev. E **50**, 1024

[22] H. van Beijeren, R. Kutner, and H. Spohn 1985 Phys. Rev. Lett. **54**, 2026

[23] D. A. Huse and C. L. Henley 1985 Phys. Rev. Lett. **54**, 2708

[24] E. Frey, U. C. Täuber, and T. Hwa 1996 Phys. Rev. E **53**, 4424

[25] J. M. Kim and J. M. Kosterlitz 1989 Phys. Rev. Lett. **62**, 2289

[26] B. M. Forrest and L.-H. Tang 1990 Phys. Rev. Lett. **64**, 1405

[27] J. G. Amar and F. Family 1990 Phys. Rev. A **41**, 3399

[28] T. Hwa and E. Frey 1991 Phys. Rev. A **44**, R7873

[29] T. Halpin-Healy 1991 Phys. Rev. A **44**, R3415

[30] J. M. Kim, M. A. Moore, and A. J. Bray 1991 Phys. Rev. A **44**, 2345

[31] P. Calabrese and P. Le Doussal 2011 Phys. Rev. Lett. **106**, 250603

[32] T. Imamura and T. Sasamoto 2012 Phys. Rev. Lett. **108**, 190603

[33] M. Prähofer and H. Spohn 2000 Phys. Rev. Lett. **84**, 4882

[34] K. Takeuchi and M. Sano 2012 J. Stat. Phys. **147**, 853

[35] K. A. Takeuchi 2013 Phys. Rev. Lett. **110**, 210604

[36] T. Halpin-Healy and Y. Lin 2014 Phys. Rev. E **89**, 010103

[37] T. Halpin-Healy 2012 Phys. Rev. Lett. **109**, 170602

[38] T. Halpin-Healy and K. A. Takeuchi 2015 J. Stat. Phys. **160**, 794

[39] S. G. Alves, T. J. Oliveira, and S. C. Ferreira 2014 Phys. Rev. E **90**, 020103(R)

[40] J. Kondev, and C. L. Henley, and D. G. Salinas 2000 Phys. Rev. E **61**, 104

[41] J. Kelling and G. Ódor 2011 Phys. Rev. E **84**, 061150

[42] S. V. Ghaisas 2006 Phys. Rev. E **73**, 022601

[43] F. D. A. Aarão Reis 2004 Phys. Rev. E **69**, 021610

[44] L.-H. Tang, B. M. Forrest, and D. E. Wolf 1992 Phys. Rev. A **45**, 7162

[45] E. Marinari, A. Pagnani, and G. Parisi 2000 J. Phys. A: Math. Gen. **33**, 8181

[46] G. Ódor, B. Liedke, and K.-H. Heinig 2010 Phys. Rev. E **81**, 031112

[47] T. Nattermann and L.-H. Tang 1992 Phys. Rev. A **45**, 7156

[48] J. P. Bouchaud and M. E. Cates 1993 Phys. Rev. E **47**, R1455

[49] Y. Tu 1994 Phys. Rev. Lett. **73**, 3109

[50] M. Schwartz and S. F. Edwards 1992 Europhys. Lett. **20**, 301

[51] M. Lässig 1998 Phys. Rev. Lett. **80**, 2366

[52] F. Colaiori and M. A. Moore 2001 Phys. Rev. Lett. **86**, 3946

[53] T. Kloss, L. Canet, and N. Wschebor 2012 Phys. Rev. E **86**, 051124

[54] T. Kloss, L. Canet, B. Delamotte, and N. Wschebor 2014 Phys. Rev. E **89**, 022108

[55] G. Palasantzas, D. Tsamouras, and J. D. Hosson 2002 Surf. Sci. **507**, 357

[56] D. Tsamouras, G. Palasantzas, and J. T. M. De Hosson 2001 Appl. Phy. Lett. **79**

[57] R. A. L. Almeida, S. O. Ferreira, T. J. Oliveira, and F. D. A. Aarão Reis 2014 Phys. Rev. B **89**, 045309

[58] Pagnani, A. and Parisi, G. 2015 Phys. Rev. E **92**, 010101

[59] C.-S. Chin and M. den Nijs 1999 Phys. Rev. E **59**, 2633

[60] T. Singha and M. K. Nandy 2014 Phys. Rev. E **90**, 062402

[61] V. Yakhot and S. Orszag 1986 J. Sci. Comput. **1**, 3

[62] T. Singha and M. K. Nandy. J. Stat. Mech. (2015) P05020

[63] J. P. Doherty, M. A. Moore, J. M. Kim, and A. J. Bray 1994 Phys. Rev. Lett **72** 2041

[64] V. G. Miranda and F. D. A. Aarão Reis 2008 Phys. Rev. E **77**, 031134

[65] T. Halpin-Healy and G. Palasantzas 2014 Europhys. Lett. **105** 50001

[66] B. Derrida and C. Appert 1999 J. Stat. Phys. **94**, 1

[67] N. Chia and R. Bundschuh 2005 Phys. Rev. E **72**, 051102